Atmospheric Pollution Research 6 (2015) 184-190

Atmospheric Pollution Research

www.atmospolres.com

Characterization and activity of N doped TiO_2 supported VPO catalysts for NO oxidation

Yong Jia [1], Daqian Du [1], Jiachuan Bai [1], Jie Ding [2], Qin Zhong [2], Xilou Ding [1]

[1] *School of Energy and Environment, Anhui University of Technology, Ma Anshan 243032, China*
[2] *School of Chemical Engineering, Nanjing University of Science and Technology, Nanjing 210094, China*

ABSTRACT

Nitrogen (N) doped TiO_2 supported vanadium phosphorus oxide (VPO) catalysts were prepared and tested for catalytic oxidation of NO. The experimental results showed that 0.1V(5)PO/TiN(1) was the optimal catalyst for NO oxidation and the NO conversion could reach 61% at temperature of 350 °C. The physico–chemical properties of 0.1V(5)PO/TiN(1) catalyst were characterized by Brunauer–Emmett–Teller measurements (BET), Photoluminescence (PL), X–ray photoelectron spectroscopy (XPS), Infrared spectroscopy measurements of NH_3 adsorbed on catalysts (NH_3–IR), and Infrared Fourier transform spectroscopy (FTIR). The PL and XPS spectra revealed that the oxygen storage capacity and catalytic activity of VPO/Ti catalyst can be improved by nitrogen doping. The H_2–TPR profile also indicated that V(5)PO/TiN(1) catalyst had a superior redox property. Activity test results and FTIR spectra showed that 0.1V(5)PO/TiN(1) catalysts had a superior resistivity to SO_2 and the NO oxidation rate is above 50% at temperature of 350 °C when SO_2 concentration is 200 ppm to 800 ppm.

Keywords: *NO oxidation, VPO/TiN, oxygen vacancies, surface acidity*

Corresponding Author:
Yong Jia
☎ : *+86-018355557109*
🖷 : *+86-0555-2311719*
✉ : *jiayong2000@163.com*

Article History:
Received: 15 May 2014
Revised: 27 August 2014
Accepted: 27 August 2014

doi: 10.5094/APR.2015.022

1. Introduction

Nitrogen oxides (NO_X) in flue gas generated as a result of combustion of fossil fuel in, e.g., thermal power plants, industrial boilers and some chemical plants, etc., are the main cause of global environmental problems such as acid rain and photochemical smog (Sousa et al., 2012). The process of selective catalytic reduction (SCR) with NH_3 is widely used for de–NO_X treatment of flue gases (Li et al., 2013). Although the SCR process appears effective for NO_X removal, there are still several problems such as large reactor volume, high cost and ammonia escape, etc. (Zhang et al., 2006; She and Flytzani–Stephanopoulos, 2007; Mao et al., 2008; Li et al., 2012). Accordingly, more efficient technologies are needed to meet future environmental regulations.

Wet scrubbing combined SO_2/NO_X removal process is considered to be economically most competitive and have the advantage of controlling other acidic gases and particulates at the same time (Makansi, 1990; Chien et al., 2003; Hammer and Mengel, 2005; Deshwal et al., 2008; Wu et al., 2009). Ammonia–based wet flue gas desulfurization (WFGD) process has been attracted a lot of attention in China because of its high desulfurization efficiency, no secondary pollution and useful byproducts. If SO_2 and NO_X could be removed simultaneously in ammonia–based desulfurization system after minor adjustment is made, it may be a compact and economical technology. However, among the NO_X emitted from stationary combustion sources, more than 90% of NO_X is nitric oxide (NO) which is relatively insoluble in aqueous solutions (Wu et al., 2009). The maximum absorption efficiency can be achieved when the mole ratio of NO_2 to NO_X is at 50~60% (Li et al., 2012). Accordingly, it is necessary to partially oxidize NO into more soluble NO_2 to remove NO_X by wet scrubbing methods. Among several technologies, selective catalytic oxidation (SCO) is considered to be an effective and relatively low cost approach to convert NO to NO_2 (Yung et al., 2007; Wang et al., 2010). Platinum–based catalysts used for NO oxidation has been studied extensively for their high catalytic activity and chemical stability (Li et al., 2010). However, the cost of platinum is too high. Transition metal oxide catalysts (e.g., MnO_X/TiO_2, Fe/ZSM–5, CrCe/TiO_2–PILC, CeO_2–ZrO_2, $La_{1-X}Ce_XCoO_3$) have also attracted extensive interest due to their superior properties like high catalytic activity, excellent redox property and relatively low cost (Qi and Yang, 2005; Mo et al., 2007; Wen et al., 2007; Irfan et al., 2008; Atribak et al., 2010; Wu et al., 2010). Although transition metal oxide catalysts present excellent catalytic activity for NO oxidation, they are deactivated easily in the presence of SO_2 and water vapor (H_2O) (Li et al., 2012). Therefore, the poison resistance of transition metal oxide catalysts needs to be further improved.

The direct oxidation of gaseous NO to NO_2 was proposed as the main pathway for NO_2 formation (Li et al., 2010). It was also reported that the strong surface acidity of catalyst could suppress the SO_2 oxidation (Dawody et al., 2004). Catalysts with strong surface acidity could suppress the adsorption of SO_2 which is an acidic gas. Accordingly, it might be possible to improve the anti–SO_2 performance by enhancing the surface acidity of SCO catalysts. Bond and Tahir (1991) indicated that the addition of phosphorus could enhance the acid properties of V_2O_5/TiO_2 catalyst. Vanadium phosphorus oxide (VPO) catalysts have been extensively used in various catalytic reactions due to their special surface acidity and

redox (Melanova et al., 1999; Taufiq–Yap and Saw, 2008). Each vanadium atom, being pentacoordinated with oxygen atoms, acts as a Lewis acid site and is able to bind a water molecule, completing a (distorted) octahedral coordination through a V–OH bond (Melanova et al., 1999). It is well known that –OH group has strong oxidation ability. TiO_2 is widely used as a catalyst carrier because of its chemical stability and high specific surface area. Meanwhile, it is reported that nitrogen (N) doped TiO_2 could promote the formation of oxygen vacancies on the surface of catalysts, which increases the affinity for oxygen (Li et al., 2008). Oxygen vacancies absorb oxygen to form superoxide ions which are important active species for NO oxidation.

In this work, N doped TiO_2 supported VPO catalysts (VPO/TiN) for NO oxidation were prepared and characterized. The catalytic activity of VPO/TiN catalysts and the effect of SO_2 and H_2O on NO oxidation were also investigated.

2. Experimental

2.1. Catalyst preparation

Desired amount of VPO and N–doped TiO_2 (see the Supporting Material, SM, Text S1) were mixed in some distilled water. After 1 h stirring, the mixture was kept at 70 °C for 4 h and then dried completely. Finally, the N–doped TiO_2 supported VPO catalysts were obtained after calcinating for 3 h. The catalysts were denoted as *m*V(*x*)PO/TiN(*y*), where *x* represented the molar ratio of V to P, *y* represented the molar ratio of N to Ti, *m* meant the percentage of V(*x*)PO loading, e.g. 0.1V(1)PO/TiN(1).

2.2. Catalytic activity measurement

The catalytic activity measurement is shown in the SM. (see the SM, Text S2).

2.3. Catalyst characterization

The approaches for catalyst characterization are shown in the SM. (see the SM, Text S3).

3. Results and Discussion

3.1. Catalytic activity tests

Results on NO conversion as a function of temperature over 0.1V(*x*)PO/TiN(*y*) catalysts calcined at 350 °C are presented in Figures 1 and 2. It can be seen from Figure 1 that the molar ratio of P to V (m_P/m_V) plays an important role in NO conversion. The NO conversion increases with m_P/m_V up to 1/5, when above 1/5 it decreases. In a temperature range from 250 °C to 400 °C, the NO conversion over 0.1V(5)PO/Ti catalyst is above 50%. Especially, the NO conversion over 0.1V(5)PO/Ti could reach 58% at temperature of 350 °C. The effect of N doping on NO conversion over 0.1V(5)PO/TiN(*x*) catalysts is shown in Figure 2. It is obvious that the N doping has a significant promoting effect on NO conversion when the molar ratio of N to Ti (m_N/m_{Ti}) is 1/1, especially at temperature below 300 °C. The maximum conversion of NO over 0.1V(5)PO/TiN(1) catalyst is about 61% at temperature of 350 °C. The reason may be that a maximal NO conversion is achieved at 350 °C on 0.1V(5)PO/TiN(1) and then NO conversion decreases along the thermodynamic equilibrium at temperature above 350 1 °C (Halasz et al., 1996).

SCO activity test results also show that the NO conversion decreases in the following sequence: 0.1V(5)PO/TiN(1)> 0.05V(5)PO/TiN(1)>0.2V(5)PO/TiN(1)>0.3V(5)PO/TiN(1) (see the SM, Figure S1). Accordingly, the 0.1V(5)PO/TiN(1) catalyst calcined at 350 °C was chosen for the further investigations because it's catalytic activity for NO oxidation is the highest.

3.2. Characterization of VPO/TiN catalysts

Specific surface area and pore size distribution. The specific surface area and pore size distribution of different samples are presented in Table 1. It can be seen from Table 1 that the surface area of 0.1V(5)PO/TiN(1) catalyst is 8.29$m^2\ g^{-1}$, which is 41.2% larger than that of 0.1V(5)PO/Ti sample. It indicates that the pore structure of 0.1V(5)PO/Ti catalyst could be ameliorated by N doping (see the SM, Text S4 and Figure S2). For *m*V(5)PO/TiN(1) catalysts, the surface area, pore volume and pore size of 0.1V(5)PO/TiN(1) catalyst are the greatest. The possible reason may be that the distribution of V(5)PO over TiN(1) carrier is uneven when the VPO loading is below 10%, while the pore of 0.1V(5)PO/TiN(1) catalyst would be partially blocked as the V(5)PO loading is above 10%. The larger surface area is favorable to the exposure of more active sites, thus enhancing the dual contact between NO and catalysts during oxidation. These BET results are consistent with activity test (Figure 2).

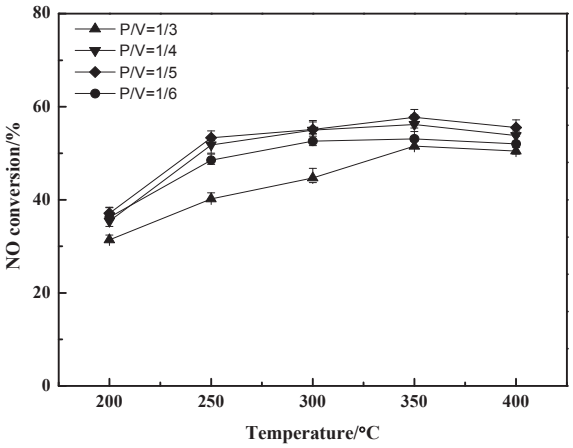

Figure 1. *NO conversion over 0.1V(x)PO/Ti catalysts at different molar ratios of P to V.*

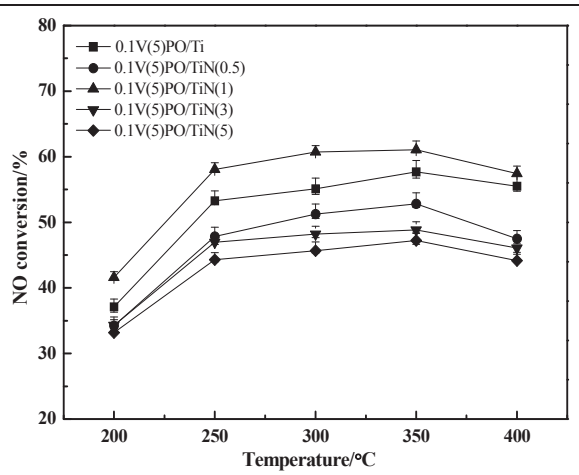

Figure 2. *NO conversion over 0.1V(5)PO/TiN(x) catalysts.*

Oxygen vacancies analysis. It is reported that N doped TiO_2 carrier could promote the formation of oxygen vacancy on the surface of catalysts, which are favorable for catalytic oxidation of NO (Li et al., 2008). Accordingly, oxygen vacancy of 0.1V(5)PO/TiN(1) catalyst was investigated by photoluminescence (PL) spectra and results are presented in Figure 3. It can be observed from Figure 3 that there are two peaks at around 465 and 523 nm respectively. The former peak could be ascribed to *F* center which obtained by trapping

double–electron oxygen vacancy ($V_O^{\cdot\cdot}$) (Cong et al., 2007), while the latter is attributed to F^+ center which obtained by trapping single–electron oxygen vacancy ($V_O^{\cdot}$) (Lei et al., 2001). Figure 3 also shows that the peak intensity at 465 nm and 523 nm of 0.1V(5)PO/TiN(1) catalyst is a little lower than that of 0.1V(5)PO/Ti sample, which indicates that the N doping could promote the formation of oxygen vacancy (Di Valentin et al., 2005; Li et al., 2013). This oxygen vacancies analysis results are consistent with the activity test in Figure 2.

Table 1. *The specific surface areas of V(5)PO/TiN(1) and V(5)PO/Ti catalysts*

Sample	Surface Area ($m^2\ g^{-1}$)	Pore Volume ($cm^3\ g^{-1}$)	Pore Size (nm)
0.05V(5)PO/TiN(1)	4.16	0.09	71.11
0.1V(5)PO/TiN(1)	8.29	0.48	114.72
0.2V(5)PO/TiN(1)	4.89	0.02	78.03
0.3V(5)PO/TiN(1)	4.56	0.02	75.85
0.1V(5)PO/Ti	5.87	0.55	120.33

XPS analysis. X–ray photoelectron spectroscopy (XPS) was used to investigate the surface characteristics of 0.1V(5)PO/TiN(1) catalyst. Photoelectron spectra of Ti *2p*, V *2p*, N *1s*, O *1s* levels are displayed in Figure 4 and surface atomic concentrations of Ti, V, N, O were summarized in Table 2.

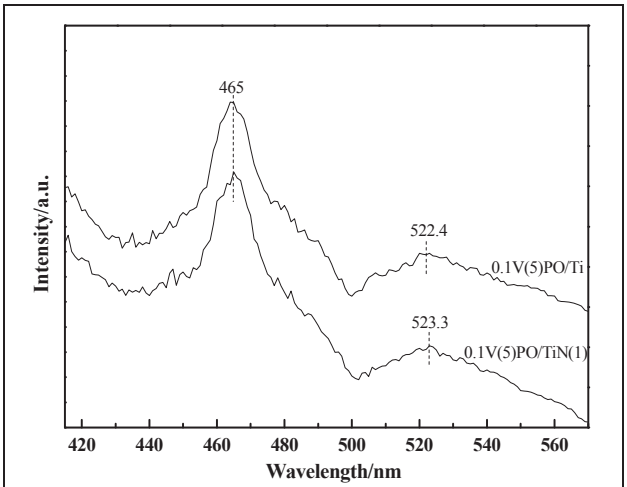

Figure 3. *PL spectra of 0.1V(5)PO/TiN(1) and 0.1V(5)PO/Ti catalysts.*

The Ti *2p* XPS spectra of 0.1V(5)PO/TiN(1) and 0.1V(5)PO/Ti are presented in Figure 4a. For 0.1V(5)PO/Ti catalyst, core level peaks of Ti $2p_{1/2}$ and Ti $2p_{3/2}$ are observed at 464.67 and 458.75 eV respectively (Reddy et al., 2006). Compared with 0.1V(5)PO/Ti, the Ti $2p_{1/2}$ and Ti $2p_{3/2}$ peaks of 0.1V(5)PO/TiN(1) sample shift to a lower binding energy by 0.1 and 0.07 eV. Lower binding energy of Ti *2p* in 0.1V(5)PO/TiN(1) catalyst could be due to the covalent bond between N and Ti (Sathish et al., 2005; Peng et al., 2008). The binding energy of Ti *2p* of 0.1V(5)PO/TiN(1) sample displays negative shift, which also indicates that the electron density is increased around titanium atoms. The reason may be that electrons combined with oxygen vacancies migrate to titanium ions (Yamada et al., 2008). Compared to oxygen, the electronegativity of nitrogen is lower, which also results in increase of electron density around Ti atoms (Wiswanathan, 2003). Accordingly, it is further confirmed that nitrogen was successfully incorporated into the TiO_2 lattice and substituted for oxygen.

Figure 4b shows the V $2p_{3/2}$ XPS spectra of 0.1V(5)PO/Ti and 0.1V(5)PO/TiN(1). For 0.1V(5)PO/Ti catalyst, the binding energies of 517.60 eV and 516.70 eV which correspond to V^{5+} and V^{4+} are displayed respectively (Zhang et al., 2009; Bayati et al., 2010). Compared to 0.1V(5)PO/Ti, the V $2p_{3/2}$ spectra shows that the binding energies of 0.1V(5)PO/TiN(1) shift to lower values. Moreover, it can also be seen from Table 2 that the surface atomic concentration of V^{5+} and V^{5+}/V of 0.1V(5)PO/TiN(1) catalyst are lower than that of 0.1V(5)PO/Ti. These results could be attributed to the electron donating effect of oxygen vacancies ($V_O^{\cdot\cdot}$, $V_O^{\cdot}$) of 0.1V(5)PO/TiN(1) catalyst (Li et al., 2013), which is consistent with H_2–TPR results (see the SM, Text S5 and Figure S3).

The N *1s* XPS spectra of 0.1V(5)PO/TiN(1) and 0.1V(5)PO/Ti are shown in Figure 4c. Compared with 0.1V(5)PO/Ti catalyst, two peaks of 0.1V(5)PO/TiN(1) at binding energies of 399.70 eV and 401.20 eV are observed. The peak at 399.7 eV could be attributed to anionic N– in O–Ti–N linkages, which has been confirmed by many researchers (Gyorgy et al., 2003; Zhang et al., 2008; Xing et al., 2009). The peak at 401.20 eV could be ascribed to the oxidized nitrogen of Ti–O–N (Xing et al., 2009). This oxidized nitrogen chemically adsorbed on the surface of 0.1V(5)PO/TiN(1) catalyst and appeared at a higher binding energy.

Figure 4d shows the O *1s* XPS spectra of 0.1V(5)PO/Ti and 0.1V(5)PO/TiN(1) catalysts. Obviously, only crystal lattice oxygen (O*β*) peak of 0.1V(5)PO/Ti sample at 530.60 eV is observed. It could also be seen from Figure 4d that crystal lattice oxygen (O*β*) peak of the 0.1V(5)PO/TiN(1) catalyst is observed at 530.48 eV, which shifts to a lower binding energy by 0.12 eV in contrast to 0.1V(5)PO/Ti sample. There are two factors that could be responsible for the binding energy shift, the oxygen vacancies and the lower electronegativity of nitrogen compared with oxygen, which could result in the increased outer electron density of O and the correspondingly decreased binding energy (Yamada et al., 2008; Xing et al., 2009). Meanwhile, it can also be seen from Figure 4d that the O *1s* XPS spectra of 0.1V(5)PO/TiN(1) catalyst has a shoulder–type peak at 531.97 eV, which is attributed to chemisorbed oxygen (Oα) (Larachi et al., 2002). However, no such shoulder–type peak is detected in O *1s* XPS spectra of 0.1V(5)PO/Ti. These are consistent with the results obtained in Table 2. It can be explained as that N doping prompted the formation of chemisorbed oxygen on the surface of 0.1V(5)PO/TiN(1) catalyst.

Surface acid sites analysis. NH_3–IR spectroscopy was employed to elucidate the acidity of 0.1V(*x*)PO/TiN(1) catalysts and the results are presented in Figure 5. It can be seen from Figure 5 that there are two absorption bands in the profiles of 0.1VO/Ti(N) and 0.1V(*x*)PO/TiN(1) catalysts. The band located at around 1 430 cm^{-1} is assigned to N–H bending vibration of NH_3 chemisorbed on Bronsted acid sites (e.g. P–OH, V–OH) (Tang et al., 2010), while the band at around 1 613 cm^{-1} could be attributed to the N–H bending vibration of NH_3 chemisorbed on Lewis acid sites (such as V=O) (Rasmussen et al., 2012). Figure 5 shows that the intensities of infrared absorption bands of Bronsted acid sites increase slightly with m_P/m_V up to 1/5, above which it decreases. The possible reason is that the amount of P–OH increased with m_P/m_V up to 1/5, above which the hydroxyl groups bonded to vanadium are obviously replaced with P–OH (Kamata et al., 1998). The acid strength of the P–OH is weaker than that of V–OH. However, there are no obvious differences in NH_3–IR spectra of Lewis acid sites at different of m_P/m_V.

Figure 6 displays the NH_3–IR spectra of V(5)PO/TiN(1) catalysts with different V(5)PO loading. Obviously, infrared absorption bands of Bronsted acid sites and Lewis acid sites are observed. With the increase of V(5)PO loading, the infrared absorption bands intensities of Bronsted acid sites decrease, while the infrared absorption bands intensities of Lewis acid sites increase. The reason may be that more hydroxyl groups bonded to vanadium are replaced with P–OH at higher V(5)PO loading, which result in parts of V–OH is transformed to V=O (Kamata et al., 1998). P–OH groups are also responsible for Bronsted acidity. However, the acid strength of the P–OH groups is weaker compared with the V–OH groups (Kamata et al., 1998).

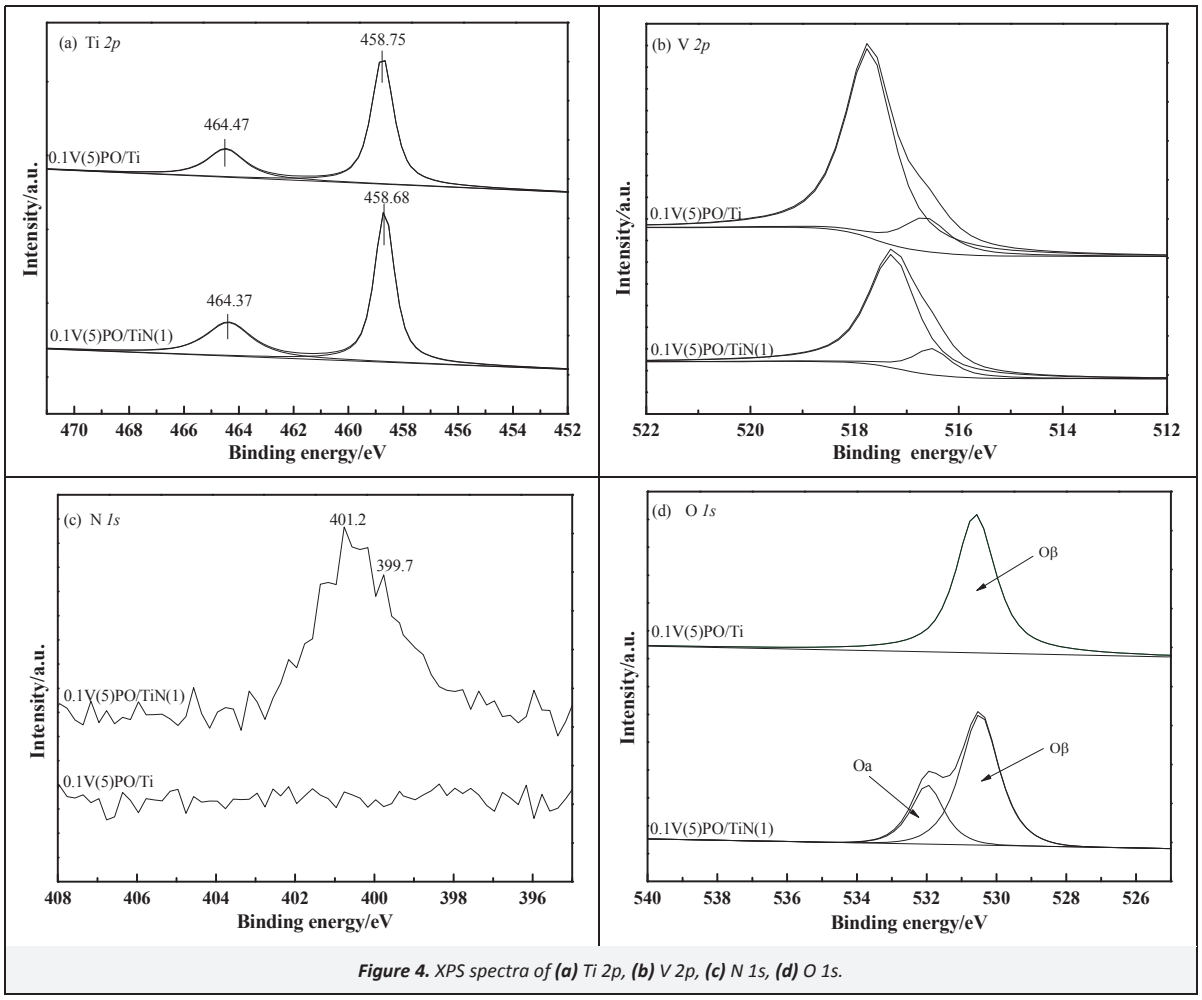

Figure 4. *XPS spectra of* ***(a)*** *Ti 2p,* ***(b)*** *V 2p,* ***(c)*** *N 1s,* ***(d)*** *O 1s.*

Table 2. *XPS results of 0.1V(5)PO/TiN(1) and 0.1V(5)PO/Ti samples*

Samples	Surfaces Atomic Concentrations (%)						Surface Atomic Ratio	
	Ti	V^{4+}	V^{5+}	N	Oα	Oβ	V^{5+}/V	Oα/O
0.1V(5)PO/TiN(1)	16.13	1.78	3.71	2.15	19.87	51.92	0.68	0.28
0.1V(5)PO/Ti	14.93	1.46	8.39		0	69.88	0.85	0

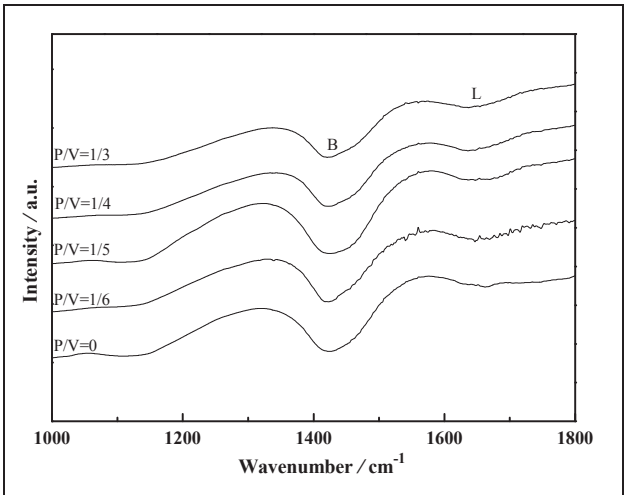

Figure 5. *NH_3–IR spectra of 0.1VPO/TiN(1) catalysts at different P/V.*

3.3. Effects of SO_2 and H_2O

The effect of SO_2 and H_2O on NO conversion over 0.1V(5)PO/TiN(1) catalyst are present in Figures 7 and 8. Figure 7 shows the NO conversion over 0.1V(5)PO/TiN(1) catalyst in the presence of 4% H_2O (by vol.) and 0.02% SO_2 (by vol.), fed either separately or simultaneously. NO oxidation conversion over 0.1V(5)PO/TiN(1) catalyst at different SO_2 concentrations are presented in Figure 8. In the presence of SO_2, Figure 7 shows that the NO conversion increases with temperature up to 250 °C, above which it decreases slightly and the NO conversion reaches almost a constant value of 51% beyond a temperature of 350 5 °C. The reason may be that NO_X was adsorbed to form intermediate nitrates on the surface of catalyst when the temperature was below 250 °C, while these intermediate nitrates decompose and the NO conversion decreases gradually along the thermodynamic equilibrium at temperature above 250 °C (Halasz et al., 1996; Yung et al., 2007; Wang et al., 2010). Moreover, Figure 8 shows that NO conversion increases slightly with SO_2 concentration increasing from 200 ppm to 800 ppm and the NO conversion is about 62% at SO_2 concentration 800 ppm, which indicates that the 0.1V(5)PO/TiN(1) catalyst has a superior resistivity to SO_2. It could be obtained from Figure 7 that

H_2O suppressed NO conversion over 0.1V(5)PO/TiN(1) catalyst. However, the NO conversion could reach almost a constant value of 45% as the temperature is above 350 °C, whether feed H_2O and SO_2 separately or simultaneously.

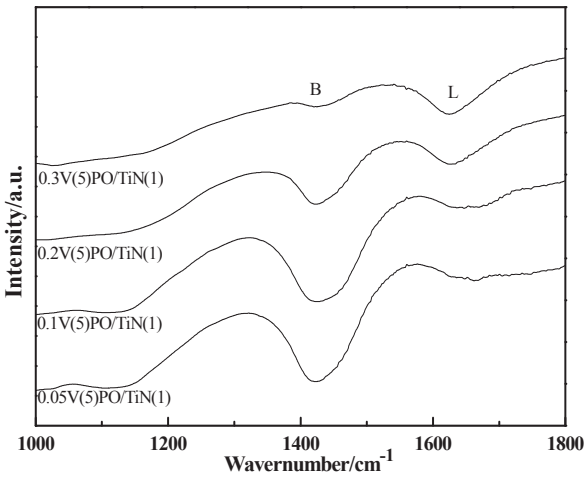

Figure 6. *NH_3–IR spectra of the V(5)PO/TiN catalysts with different V(5)PO loadings.*

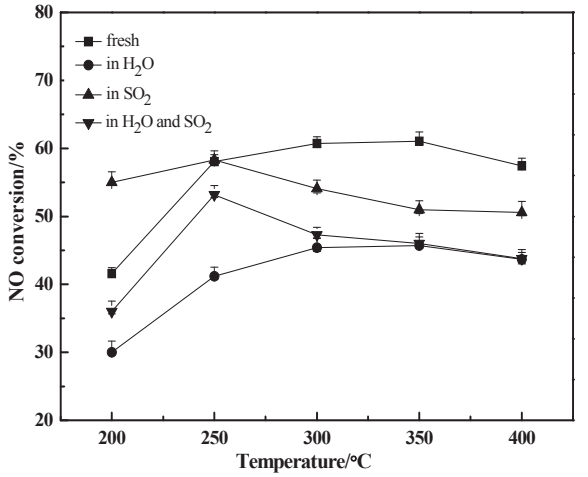

Figure 7. *The effect of H_2O and SO_2 on NO oxidation over 0.1V(5)PO/TiN(1) catalyst.*

Figure 9 shows the FTIR spectra of 0.1V(5)PO/TiN(1) catalysts (fresh and used). Obviously, there are almost no visible differences in the FTIR spectra between the used 0.1V(5)PO/TiN(1) catalyst and fresh samples. Characteristic signal of sulfate at 1 140 cm^{-1} could not be observed in Figure 9, which indicates that 0.1V(5)PO/TiN(1) catalyst has a good resistance to SO_2. The NH_3–IR spectra of 0.1V(5)PO/TiN(1) catalysts (fresh and used) are shown in Figure S4 (see the SM, Text S6 and Figure S4).

4. Conclusions

Characterization and catalytic activity of N doped TiO_2 supported VPO catalysts for NO oxidation were investigated in this paper. The experimental results showed that 0.1V(5)PO/TiN(1) catalyst calcined at 350 °C was optimum for NO oxidation. The NO conversion over 0.1V(5)PO/TiN(1) catalyst could reach 61% at temperature of 350 °C. The addition of N could improve the oxygen storage capacity and catalytic activity of VPO/Ti catalyst, which were confirmed by PL, XPS and TPR analysis. Activity test results show that SO_2 had a slight influence on the NO conversion over 0.1V(5)PO/TiN(1) catalyst. FTIR spectra presents that there was no characteristic peaks of sulfate on the surface of 0.1V(5)PO/TiN(1) used in the presence of SO_2 and H_2O. It was indicated that SO_2 adsorption and the sulfation of vanadium were restrained because of the surface acidity of 0.1V(5)PO/TiN(1). Both activity test and characterization results show that 0.1V(5)PO/TiN(1) catalyst had a superior resistance to SO_2. H_2O could suppress the NO oxidation over 0.1V(5)PO/TiN(1) catalyst and corresponding mechanism needs to be further investigated.

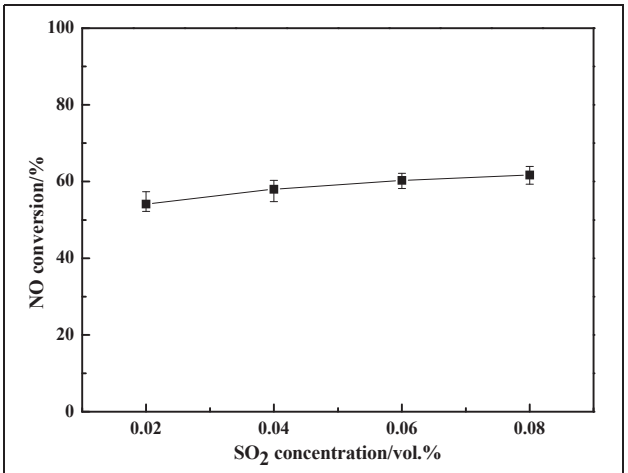

Figure 8. *The effect of SO_2 concentration on NO oxidation over 0.1V(5)PO/TiN(1) catalyst.*

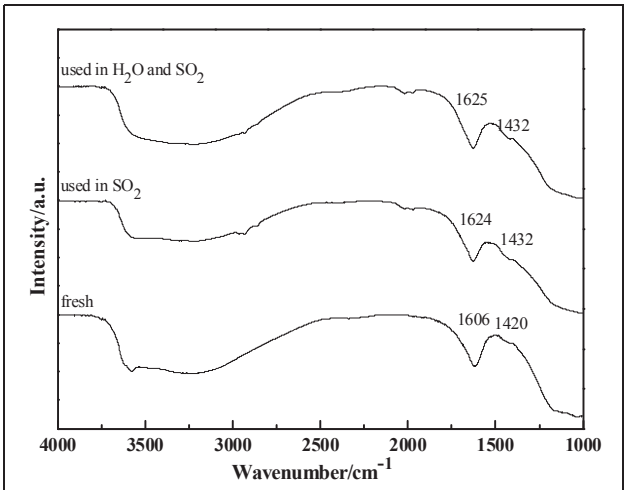

Figure 9. *FTIR spectra of 0.1V(5)PO/TiN(1) catalysts.*

Acknowledgments

This work was financially supported by the National Natural Science Foundation of China (51308002) and School Youth Fund (QZ201309).

Supporting Material Available

Preparation of VPO and TiN (text), Catalytic activity measurement (text), catalyst characterization (text), Influence of V(5)PO loading on NO conversion (Figure S1), Scanning electron microscopy (SEM) analysis (text and Figure S2), The H_2–TPR profiles (Figure S3), The NH_3–IR spectra of used 0.1V(5)PO/TiN(1) (text and

Figure S4). This information is available free of charge via the internet at http://www.atmospolres.com.

References

Atribak, I., Guillen–Hurtado, N., Bueno–Lopez, A., Garcia–Garcia, A., 2010. Influence of the physico–chemical properties of CeO_2–ZrO_2 mixed oxides on the catalytic oxidation of NO to NO_2. *Applied Surface Science* 256, 7706–7712.

Bayati, M.R., Golestani–Fard, F., Moshfegh, A.Z., 2010. Photo–degradation of methelyne blue over V_2O_5–TiO_2 nano–porous layers synthesized by micro arc oxidation. *Catalysis Letters* 134, 162–168.

Bond, G.C., Tahir, S.F., 1991. Vanadium–oxide monolayer catalysts – Preparation, characterization and catalytic activity. *Applied Catalysis* 71, 1–31.

Chien, T., Chu, H., Hsueh, H., 2003. Kinetic study on absorption of SO_2 and NO_X with acidic $NaClO_2$ solutions using the spraying column. *Journal of Environmental Engineering* 129, 967–974.

Cong, Y., Zhang, J.L., Chen, F., Anpo, M., 2007. Synthesis and characterization of nitrogen–doped TiO_2 nanophotocatalyst with high visible light activity. *Journal of Physical Chemistry C* 111, 6976–6982.

Dawody, J., Skoglundh, M., Fridell, E., 2004. The effect of metal oxide additives (WO_3, MoO_3, V_2O_5, Ga_2O_3) on the oxidation of NO and SO_2 over Pt/Al_2O_3 and $Pt/BaO/Al_2O_3$ catalysts. *Journal of Molecular Catalysis A–Chemical* 209, 215–225.

Deshwal, B.R., Jin, D.S., Lee, S.H., Moon, S.H., Jung, J.H., Lee, H.K., 2008. Removal of NO from flue gas by aqueous chlorine–dioxide scrubbing solution in a lab–scale bubbling reactor. *Journal of Hazardous Materials* 150, 649–655.

Di Valentin, C., Pacchioni, G., Selloni, A., 2005. Theory of carbon doping of titanium dioxide. *Chemistry of Materials* 17, 6656–6665.

Gyorgy, E., del Pino, A.P., Serra, P., Morenza, J.L., 2003. Depth profiling characterisation of the surface layer obtained by pulsed Nd: YAG laser irradiation of titanium in nitrogen. *Surface & Coatings Technology* 173, 265–270.

Halasz, I., Brenner, A., Ng, K.Y.S., Hou, Y., 1996. Catalytic activity and selectivity of H–ZSM5 for the reduction of nitric oxide by propane in the presence of oxygen. *Journal of Catalysis* 161, 359–372.

Hammer, M.T., Mengel, M.L., 2005. *Flue Gas Desulfurization Process and Apparatus for Removing Nitrogen Oxides*, Patent US 6958133 B2.

Irfan, M.F., Goo, J.H., Kim, S.D., 2008. Co_3O_4 based catalysts for NO oxidation and NO_x reduction in fast SCR process. *Applied Catalysis B: Environmental* 78, 267–274.

Kamata, H., Takahashi, K., Odenbrand, C.U.I., 1998. Surface acid property and its relation to SCR activity of phosphorus added to commercial $V_2O_5(Wo_3)/TiO_2$ catalyst. *Catalysis Letters* 53, 65–71.

Larachi, F.C., Pierre, J., Adnot, A., Bernis, A., 2002. Ce 3d XPS study of composite $Ce_xMn_{1-x}O_{2-y}$ wet oxidation catalysts. *Applied Surface Science* 195, 236–250.

Lei, Y., Zhang, L.D., Meng, G.W., Li, G.H., Zhang, X.Y., Liang, C.H., Chen, W., Wang, S.X., 2001. Preparation and photoluminescence of highly ordered TiO_2 nanowire arrays. *Applied Physics Letters* 78, 1125–1127.

Li, H.Y., Zhang, S.L., Zhong, Q., 2013. Effect of nitrogen doping on oxygen vacancies of titanium dioxide supported vanadium pentoxide for ammonia–SCR reaction at low temperature. *Journal of Colloid and Interface Science* 402, 190–195.

Li, K., Tang, X.L., Yi, H.H., Ning, P., Kang, D.J., Wang, C., 2012. Low–temperature catalytic oxidation of NO over Mn–Co–Ce–Ox catalyst. *Chemical Engineering Journal* 192, 99–104.

Li, L., Shen, Q., Cheng, J., Hao, Z., 2010. Catalytic oxidation of NO over TiO_2 supported platinum clusters. II: Mechanism study by in situ FTIR spectra. *Catalysis Today* 158, 361–369.

Li, Y.X., Ma, G.F., Peng, S.Q., Lu, G.X., Li, S.B., 2008. Boron and nitrogen co–doped titania with enhanced visible–light photocatalytic activity for hydrogen evolution. *Applied Surface Science* 254, 6831–6836.

Makansi, J., 1990. Will combined SO_2/NO_X processes find a niche in the market. *Power* 134, 26–28.

Mao, Y.P., Bi, W., Long, X.L., Xiao, W.D., Li, W., Yuan, W.K., 2008. Kinetics for the simultaneous absorption of nitric oxide and sulfur dioxide with the hexamminecobalt solution. *Separation and Purification Technology* 62, 183–191.

Melanova, K., Benes, L., Vlcek, M., Patrono, P., Massucci, M.A., Galli, P., 1999. Preparation and characterization of vanadyl phosphates modified with two trivalent metal cations. *Materials Research Bulletin* 34, 895–903.

Mo, J.H., Tong, Z.Q., Zhang, J.F., 2007. Performance of Mn/Co–Ba–Al–O for catalytic oxidation of nitric oxide. *Acta Scientiae Circumstantiae* 27, 1793–1798.

Peng, F., Cai, L.F., Yu, H., Wang, H.J., Yang, J., 2008. Synthesis and characterization of substitutional and interstitial nitrogen–doped titanium dioxides with visible light photocatalytic activity. *Journal of Solid State Chemistry* 181, 130–136.

Qi, G.S., Yang, R.T., 2005. Selective catalytic oxidation (SCO) of ammonia to nitrogen over Fe/ZSM–5 catalysts. *Applied Catalysis A–General* 287, 25–33.

Rasmussen, S.B., Mikolajska, E., Daturi, M., Banares, M.A., 2012. Structural characteristics of an amorphous VPO monolayer on alumina for propane ammoxidation. *Catalysis Today* 192, 96–103.

Reddy, B.M., Rao, K.N., Reddy, G.K., Bharah, P., 2006. Characterization and catalytic activity of V_2O_5/Al_2O_3–TiO_2 for selective oxidation of 4–methylanisole. *Journal of Molecular Catalysis A–Chemical* 253, 44–51.

Sathish, M., Viswanathan, B., Viswanath, R.P., Gopinath, C.S., 2005. Synthesis, characterization, electronic structure, and photocatalytic activity of nitrogen–doped TiO_2 nanocatalyst. *Chemistry of Materials* 17, 6349–6353.

She, X., Flytzani–Stephanopoulos, M., 2007. Activity and stability of Ag–alumina for the selective catalytic reduction of NO_X with methane in high–content SO_2 gas streams. *Catalysis Today* 127, 207–218.

Sousa, J.P.S., Pereira, M.F.R., Figueiredo, J.L., 2012. NO oxidation over nitrogen doped carbon xerogels. *Applied Catalysis B–Environmental* 125, 398–408.

Tang, F.S., Xu, B.L., Shi, H.H., Qiu, J.H., Fan, Y.N., 2010. The poisoning effect of Na^+ and Ca^{2+} ions doped on the V_2O_5/TiO_2 catalysts for selective catalytic reduction of NO by NH_3. *Applied Catalysis B–Environmental* 94, 71–76.

Taufiq–Yap, Y.H., Saw, C.S., 2008. Effect of different calcination environments on the vanadium phosphate catalysts for selective oxidation of propane and *n*–butane. *Catalysis Today* 131, 285–291.

Wang, H.Q., Wang, J., Wu, Z.B., Liu, Y., 2010. NO catalytic oxidation behaviors over $CoOx/TiO_2$ catalysts synthesized by Sol–Gel method. *Catalysis Letters* 134, 295–302.

Wen, Y., Zhang, C., He, H., Yu, Y., Teraoka, Y., 2007. Catalytic oxidation of nitrogen monoxide over $La_{1-x}Ce_xCoO_3$ perovskites. *Catalysis Today* 126, 400–405.

Wiswanathan, B., 2003. Photocatalytic processes – selection criteria for the choice of materials. *Bulletin of the Catalysis Society of India* 2, 71–74.

Wu, Z.B., Tang, N.A., Xiao, L., Liu, Y., Wang, H.C., 2010. MnO_x/TiO_2 composite nanoxides synthesized by deposition–precipitation method as a superior catalyst for NO oxidation. *Journal of Colloid and Interface Science* 352, 143–148.

Wu, Z.B., Sheng, Z.Y., Liu, Y., Wang, H.Q., Tang, N., Wang, J., 2009. Characterization and activity of Pd–modified TiO_2 catalysts for photocatalytic oxidation of NO in gas phase. *Journal of Hazardous Materials* 164, 542–548.

Xing, M., Zhang, J., Chen, F., 2009. New approaches to prepare nitrogen–doped TiO_2 photocatalysts and study on their photocatalytic activities in visible light. *Applied Catalysis B: Environmental* 89, 563–569.

Yamada, K., Yamane, H., Matsushima, S., Nakamura, H., Ohira, K., Kouya, M., Kumada, K., 2008. Effect of thermal treatment on photocatalytic

activity of N–doped TiO_2 particles under visible light. *Thin Solid Films* 516, 7482–7487.

Yung, M.M., Holmgreen, E.M., Ozkan, U.S., 2007. Cobalt–based catalysts supported on titania and zirconia for the oxidation of nitric oxide to nitrogen dioxide. *Journal of Catalysis* 247, 356–367.

Zhang, X., Li, X., Wu, J., Yang, R., Zhang, Z., 2009. Selective catalytic reduction of NO by ammonia on V_2O_5/TiO_2 catalyst prepared by Sol–Gel method. *Catalysis Letters* 130, 235–238.

Zhang, G., Ding, X.M., He, F.S., Yu, X.Y., Zhou, J., Hu, Y.J., Xie, J.W., 2008. Preparation and photocatalytic properties of TiO_2–montmorillonite doped with nitrogen and sulfur. *Journal of Physics and Chemistry of Solids* 69, 1102–1106.

Zhang, H., Tong, H.L., Wang, S.J., Zhuo, Y.Q., Chen, C.H., Xu, X.C., 2006. Simultaneous removal of SO_2 and NO from flue gas with calcium–based sorbent at low temperature. *Industrial & Engineering Chemistry Research* 45, 6099–6103.